Inorg. Chem. **2005**, *44*, 7423–7430

$KBi_{2-x}Pb_x$ ($0 < x \leq 1$): A Zintl Phase Evolving from a Distortion of the Cubic Laves-Phase Structure

Siméon Ponou,[†] Noémi Müller,[†] Thomas F. Fässler,*[,†] and Ulrich Häussermann[‡]

Department Chemie, Technische Universität München, Lichtenbergstrasse 4, D-85747 Garching, Germany, and Inorganic Chemistry, Stockholm University, SE−10691 Stockholm, Sweden

Received April 19, 2005

The quasibinary system $KBi_{2-x}Pb_x$ has been investigated, both experimentally and theoretically. Phases with compositions $0 \leq x \leq 1.2$ were synthesized and structurally characterized by X-ray diffraction experiments. For low values of x ($0 \leq x < 0.6$), $KBi_{2-x}Pb_x$ adopts the cubic Laves-phase structure $MgCu_2$ (space group $Fd\bar{3}m$), which contains a rigid framework of corner-condensed symmetry-equivalent tetrahedra formed by randomly distributed Bi and Pb atoms. For compositions $x \geq 0.6$, these tetrahedra become alternately elongated and contracted. The distortion of the framework lowers the space-group symmetry to $F\bar{4}3m$ ($KBi_{1.2}Pb_{0.8}$, $F\bar{4}3m$, $Z = 8$, $a = 9.572(1)$ Å). Magnetometer measurements show that KBi_2 ($x = 0$) is metallic and goes through a superconducting transition below 3.5 K. First principles calculations reveal that the $Fd\bar{3}m \rightarrow F\bar{4}3m$ distortion is largest for KBiPb ($x = 1.0$), which at the same time turns into a semiconductor. Thus, $F\bar{4}3m$ KBiPb corresponds to a proper charge-balanced Zintl phase, $K^+[BiPb]^-$, with separated polyanionic tetrahedra, $(Bi_2Pb_2)^{2-}$. However, it was not possible to prepare $F\bar{4}3m$ KBiPb. Syntheses attempting to increase the Pb content in $KBi_{2-x}Pb_x$ above $x = 0.8$ yielded additional, not yet characterized, ternary phases.

1. Introduction

Laves phases are ubiquitous among intermetallic AB_2 systems. Far more than 1000 binary and quasibinary compounds are reported to crystallize in one of the three primary Laves-phase structure types, $MgCu_2$, $MgZn_2$, or $MgNi_2$.[1] These structures are intimately related and represent close-packed arrangements of differently sized spheres in the ratio 1:2 (topological close-packings). Characteristically, A- and B-type atoms attain high coordination numbers (A, 12B + 4A; B, 6B + 6A), and the great majority of Laves phases are transition metal systems. The formation of Laves phases is certainly strongly dependent on the size ratio of the A and B component. However, the ideal radius ratio, r_A/r_B, of 1.225 is frequently violated and known values range from 1.05 to 1.67.[2]

Only a few examples for Laves phases exist, which are exclusively composed of main group metals (i.e., s−p bonded systems). These are (a) combinations of a heavier alkali or alkaline earth metal with a lighter alkali metal or Mg (KNa_2, CsK_2, $BaNa_2$, $CaLi_2$, $BaMg_2$, $SrMg_2$, $CaMg_2$), which all display the hexagonal $MgZn_2$ structure; (b) $CaAl_2$ with the cubic $MgCu_2$ structure; and (c) compounds between heavier alkali metals and Pb or Bi (KPb_2 ($MgZn_2$ type), KBi_2, $RbBi_2$, $CsBi_2$ (all $MgCu_2$ type)). Whereas the group a compounds might be considered to be typical Laves phase systems, cases b and c appear peculiar. This is because of the rather large electronegativity difference between the A and B components, which implies a notable charge transfer leading to a formal reduction of the B component by the electropositive A metal. As a result, one could expect the formation of a polyanionic framework composed of B atoms, as known for polar intermetallics or Zintl phases. However, the polyanionic networks of polar intermetallics and Zintl phases predominantly realize localized multicenter or two-center bonding and have, in general, a lower connectivity than the B atom substructure in Laves phases. The former compounds often conform to valence rules (i.e., are charge-balanced), while the groups b and c Laves phases have to be considered as fully delocalized metallic systems.

* To whom correspondence should be addressed. E-mail: thomas.faessler@lrz.tum.de.
[†] Technische Universität München.
[‡] Stockholm University.

(1) Villars, P. *Pearsons Handbook of Crystallographic Data for Intermetallic Phases, Desk Edition*; The Material Information Society: Materials Park, OH, 1997.
(2) Hume-Rothery, W.; Smallman, R. E.; Haworth, C. W. *The Structure of Metals and Alloys*, 5th ed.; Antony Rowe Ltd.: Chippenham, U.K., 1969.

10.1021/ic050603h CCC: $30.25
Published on Web 09/22/2005

Although s−p-bonded polar intermetallic-like Laves phases cannot be rationalized by simple electron counting rules, there is a clear relationship between the valence electron concentration (vec, number of valence electrons per formula unit) and the particular Laves-phase structure that is adopted. This was shown in our recent work where we investigated in detail the pseudobinary system $CaAl_{2-x}Mg_x$.[3] With an increasing x value (decreasing electron concentration), the sequence of Laves-phase structures $MgCu_2 \rightarrow MgNi_2 \rightarrow MgZn_2$ with distinct vec stability ranges occurs. Very similar ranges are observed in the $CaAl_{2-x}Li_x$[4] and $AeAl_{2-x}Mg_x$ (Ae = Sr, Ba)[5] systems, although size effects prohibit the formation of the $MgCu_2$ type for the latter.

In this work, we report on pseudobinary $KBi_{2-x}Pb_x$ which represents another system where substitution of one atom type by another with similar size allows the study of electronic factors stabilizing Laves-phase structures. We expected behavior similar to that of the $CaAl_{2-x}Mg_x$ system (i.e., the occurrence of a $MgNi_2$-type phase between $MgCu_2$-type KBi_2 and $MgZn_2$-type KPb_2). Surprisingly, we discovered a unique structural distortion of the cubic $MgCu_2$ structure. The rigid B (Bi, Pb) atom network consisting of corner-condensed symmetry-equivalent tetrahedra changes for $x \geq 0.6$ into a network composed of compressed and elongated tetrahedra. This distortion represents the onset of an unprecedented direct transition from a fully delocalized metallic Laves KBi_2 to a charge-balanced Zintl phase, $K^+[PbBi]^-$, containing discrete polyanionic tetrahedra.

2. Experimental Section

Synthesis. Phases $KBi_{2-x}Pb_x$ were prepared from reaction mixtures where $x = 0$, 0.2, and 0.4−1.2 in steps of 0.1 of pure elements in sealed niobium ampules. The mixtures were heated at 150 °C/h to 600 °C, held at 600 °C for 10 h, and cooled at 150 °C/h to room temperature. For $x = 0$, a small amount of elemental Bi was observed in the reaction product; for $x > 0.8$, the reaction product turned into a mixture of $KBi_{2-x}Pb_x$ and additional ternary products with various K content which could not yet be structurally and compositionally characterized. All products obtained were crystalline and exhibited a gray color and metallic luster.

The $KBi_{2-x}Pb_x$ phases were characterized by their X-ray powder diffraction patterns measured on a STADI P2 equipped with Cu Kα radiation and by EDX (energy-disperse X-ray) compositional analysis in a JEOL 820 scanning electron microscope. Lattice parameters of $KBi_{2-x}Pb_x$ (at 293 K) were obtained from the least-squares refinement of the same 14 lines in the indexed powder pattern of each product (Si was taken as internal standard): a (Å) = 9.5214(4), 9.5191(6), 9.5232(7), 9.5175(3), 9.565(7), 9.569(1), 9.5716(3), 9.577(2), 9.5785(3), 9,568(2), 9,566(6) for the reaction mixtures $x = 0$, 0.2, and 0.4−1.2 in steps of 0.1, respectively (Figure 3).

X-ray Structure Determination. Single crystals of KBi2 were obtained from the reaction of stoichiometric amounts of K and Bi as described above, and a crystal of irregular habitus was mounted in a glass capillary. The lattice constants measured on a STOE IPDS diffractometer equipped with an image plate detector at 293 K were slightly smaller than the one determined from the powdered samples. Intensity data for $K(Pb,Bi)_2$ were collected from a single crystal obtained from the reaction of K/Pb/Bi in the ratio 1:0.8:1.2 ($x = 0.8$). Lattice constants measured on a Siemens SMART diffractometer equipped with a CCD detector at 293 K (9.572(1) Å) were in good agreement with the one determined from powdered samples. Qualitative EDX analyses of crystallites from the $x = 0.8$ reaction product revealed the presence of the three elements K, Bi, and Pb. The similar scattering factors of Pb and Bi preclude a possible detection of Pb/Bi ordering by X-ray diffraction. No attempt was made to refine the Pb/Bi ratio from crystallographic data. Details and results of the crystal structure investigations are given in Tables 1−3.

Table 1. Crystallographic Data and Structure Refinement for $K(Pb,Bi)_2$

empirical formula	$K(Pb,Bi)_2$
fw (g mol^{-1})	453.48
temp (K)	293
wavelength (Å)	0.71073
data collection	Siemens SMART
cryst syst	cubic
space group (No.)	$F\bar{4}3m$ (216)
unit cell dimensions (Å)	$a = 9.572(1)$
vol (Å)^3	877.0(2)
Z	8
density$_{calcd}$ (g cm^{-3})	6.869
abs coeff (mm^{-1})	77.40
abs correction	SADABS (empirical)
$F(000)$	1464
cryst size (mm^3)	0.08 × 0.13 × 0.20
Θ range for data collection (deg)	3.69−34.77
index ranges	$-15 \leq h \leq 14$ $-14 \leq k \leq 14$ $-14 \leq l \leq 12$
reflns collected	2491
independent reflns	230 [$R_{int} = 0.2017$]
reflns [$I > 2\sigma(I)$]	230
parameters	7
GOF on F^2	1.075
final R indices	R1 = 0.053, wR$_2$ = 0.107
R indices (all data)	R1 = 0.068, wR$_2$ = 0.111
refinement method	full-matrix least-squares on F^2
extinction coeff	0.0008(2)
largest diff. peak and hole (e Å$^{-3@}$	2.135 and −3.239
max shift	0.0000, 0.0000
weighting scheme	a = 0.0365 b = 0.0000
absolute structure parameter	0.25(12)

Table 2. Position Parameters

	Wyckoff	x	y	z	$U_{(eq)}$ (×10^3)
KBi_2	origin $\bar{3}$m				
K(1)	8a	1/8	1/8	1/8	43(6)
Bi	16d	1/2	1/2	1/2	34(2)
KBi_2	origin $\bar{4}3$m				
K(1)	8a	0	0	0	43(6)
Bi	16d	5/8	5/8	5/8	34(2)
$K(Pb,Bi)_2$	origin $\bar{4}3$m				
K(1)	4a	0	0	0	36(4)
K(2)	4c	1/4	1/4	1/4	31(3)
(Pb,Bi)	16e	0.6332(1)	0.6332 (1)	0.6332(1)	25(1)

Magnetic Measurements. Magnetic susceptibility measurements of KBi_2 were performed using a SQUID Magnetometer (Quantum Design MPMS 5S). The sample was cooled in the absence of a magnetic field; data were recorded after the introduction of a 10 G field, while the sample was warmed ("shielding") and then cooled ("Meissner"). A superconducting state below $T_c = 3.5$ K was observed by a sharp transition from negative to positive values of the magnetization and vice versa.

(3) Amerioun, S.; Simak, S. I.; Häussermann, U. *Inorg. Chem.* **2003**, *42*, 1467.
(4) Nesper, R.; Miller, G. *J. Alloys. Compd.* **1993**, *197*, 109.
(5) Amerioun, S.; Yokosawa, T.; Lidin, S.; Häussermann, U. *Inorg. Chem.* **2004**, *43*, 4751.

Table 3. Selected Distances in Angstroms

KBi_2[13]				$K(Pb,Bi)_2$			
Bi	−Bi	3.367(1)	6×	B	−B	3.162(1)	3×
					−B	3.607(1)	3×
	−K	3.948(1)	6×		−K(1)	3.994(1)	3×
					−K(2)	3.947(1)	3×
K	−Bi	3.948(1)	12×	K(1)	−B	3.994(1)	12×
	−K	4.123(1)	4×		−K2	4.145(1)	4×
				K(2)	−B	3.947(1)	12×
					−K(1)	4.145(1)	4×

Electronic Structure Calculations. Total energy calculations for $KBi_{2-x}Pb_x$ ($0 \le x \le 1$) were performed with the full-potential linearized augmented plane wave (FLAPW) method as implemented in the program WIEN97.[6] In full-potential techniques within density functional theory basis functions, electron densities and potentials are calculated without any shape approximation. These methods are the most accurate ones to date concerning studies of structural stability. In particular, we used well-converged plane wave sets with a cutoff parameter $R_{mt}K_{max} = 8.0$ for all elements. The Bi/Pb 5d and K 3s and 3p states were considered to be local orbitals. Exchange and correlation effects were treated by the generalized gradient approximation (GGA) according to Perdew, Burke, and Ernzerhof.[7] The reciprocal space integrations were performed with the tetrahedron method using 47 *k* points in the irreducible part of the Brillouin zone. To ensure a total energy convergence within 1 meV/formula unit, several standard tests were carried out, such as the effect of increasing the number of *k* points used in the summation over the BZ, etc.

Bi/Pb disorder was taken into account within the so-called virtual-crystal approximation (VCA), which is the simplest approximation in the hierarchy of mean-field approaches.[8,9] The network position occupied randomly by Bi and Pb atoms was treated as a fictitious atom with the nuclear charge $Z = xZ_{Pb} + (1 - x)Z_{Bi}$ (where Z_X is the corresponding nuclear charge of the pure element X) and a corresponding number of valence electrons as to force charge neutrality. The mean-field treatment is sufficient to describe the case of randomly distributed atoms,[8,9,10] and in particular, it has been shown that VCA is a suitable approximation for calculating the electronic structure of alloys between neighboring elements in the periodic table.[11,12]

3. Results

X-ray structure determination of a single crystal of KBi_2[13] confirms space group symmetry $Fd\bar{3}m$[14] and thus the $MgCu_2$ type. The lattice parameter is 9.5223(2) Å, which is very close to the value recently found in the structure re-evaluation by Emmerling et al. (9.521(2) Å).[15] K and Bi atoms are located on the sites 8a (0,0,0) and 16d (5/8, 5/8, 5/8), respectively (origin at −43 m). The structure consists of vertex sharing tetrahedra of Bi atoms, whose centers form a diamond lattice. A second diamond lattice is formed by K atoms and penetrates the one formed by the tetrahedral units (Figure 1a). Alternatively, the structure can be described as stacking of Kagomé nets of Bi atoms (Figure 1b). The cubic stacking sequence ABC of the nets leads exclusively to vertex-sharing tetrahedra. Each Bi atom is coordinated to six further Bi atoms at a distance of 3.367 Å and to six K atoms at a distance of 3.948 Å. The resulting coordination polyhedron is best described as a distorted icosahedron.[16] Each K atom coordinates 12 Bi atoms at equal distances and 4 K atoms at longer distances (4.123 Å). The K atoms are located above the four hexagon faces of the capped tetrahedron of the 12 Bi atoms. The resulting Friauf polyhedron around K is shown in Figure 2a.

Subsequent substitution of Bi by Pb in $KBi_{2-x}Pb_x$ leaves the cubic lattice constant *a* virtually unchanged until *x* reaches 0.5−0.6. At higher Pb content ($x = 0.6-0.8$), a sudden increase of *a* by approximately 0.05 Å is observed (Figure 3) along with the appearance of additional reflections in the powder patterns (Figure 4). Reactions attempting to further increase the Pb content (nominal composition $0.9 < x < 1.2$) in $KBi_{2-x}Pb_x$ did not result in significantly changed lattice parameters compared to those for $x = 0.8$ (cf. Figure 3). This is consistent with the formation of small amounts of other phases. For $x > 1.2$, the formation of other binary or ternary products is observed to a larger extent. Therefore, we concluded that the maximum value of *x* in $KBi_{2-x}Pb_x$ is around 0.8, which is also confirmed by the compositional analysis of single crystals in the composition range of $0.6 \le x \le 1.2$ by the energy-disperse X-ray (EDX) method. These analyses, however, were difficult to perform because of the extreme sensitivity of $KBi_{2-x}Pb_x$ to moisture, which rapidly increases with increasing *x*.

The extra reflections which appear in the X-ray powder pattern of $KBi_{2-x}Pb_x$ ($x \ge 0.6$) can be interpreted by a reduction of the symmetry of the cubic system upon going from $Fd\bar{3}m$ to $F\bar{4}3m$. Single crystals showing the lower symmetry $F\bar{4}3m$ were isolated from the reaction K/Bi/Pb = 1:1.2:0.8 (i.e., $x = 0.8$). Symmorphic $F\bar{4}3m$ represents a t2 subgroup of nonsymmorphic $Fd\bar{3}m$. In lower symmetric $F\bar{4}3m$, the position of the K atoms (8a in $Fd\bar{3}m$) splits into two independent positions, 4a (0,0,0) and 4c (1/4,1/4,1/4), and the rigid site 16d (5/8, 5/8, 5/8) in $Fd\bar{3}m$ occupied by the Bi atoms transforms into the site 16e (*x*, *x*, *x*) with a variable positional *x* parameter (cf. Table 2). The change from $x = 0.625$ in $Fd\bar{3}m$ to $x = 0.6332$ in $F\bar{4}3m$ causes the original Bi network to be constructed by two types of B4 tetrahedra: larger tetrahedral units shown in gray in Figure 1 and smaller ones indicated as darker units. Note that the distorted B (Bi/Pb) atom framework is still built up by a

(6) Blaha, P.; Schwarz, K.; Luitz, J. *Program WIEN97*: *A Full Potential Linearized Augmented Plane Wave Package for Calculating Crystal Properties*; Technische Universität Wien: Wien, Austria, 1999 (ISBN 3-9501031-0-4).
(7) Perdew, J. P.; Burke, S.; Ernzerhof, M. *Phys. Rev. Lett.* **1996**, *77*, 3865.
(8) Faulkner, J. S. *Prog. Mater. Sci.* **1982**, *27*, 3.
(9) Ducastelle F. *Order and Phase Stability in Alloys*; North-Holland: Amsterdam, 1991.
(10) Abrikosov, I. A.; Johansson, B. *Phys. Rev. B* **1998**, *57*, 14164.
(11) Abrikosov, I. A.; James, P.; Eriksson, O.; Söderlind, P.; Ruban, A. V.; Skriver, H. L.; Johansson, B. *Phys. Rev. B* **1996**, *54*, 3380.
(12) Hausserman, U.; Simak, S. I.; Abriksov, I. A.; Johansson, B.; Lidin, S. *J. Am. Chem. Soc.* **1998**, *120*, 10136−10146.
(13) Kronseder, C. Dissertation ETH No. 12693; ETH: Zürich, 1998.
(14) Zintl, E.; Harder, A. *Z. Phys. Chem.* **1932**, *16B*, 206.
(15) Emmerling, F.; Langin, N.; Petri, D.; Kroeker, M.; Röhr, C. *Z. Anorg. Allg. Chem.* **2004**, *630*, 171−178.
(16) Fässler, T. F.; Hoffmann, S. D. *Angew. Chem.* **2004**, *116*, 6400−6406; *Angew. Chem., Int. Ed.* **2004**, *43*, 6242−6247.

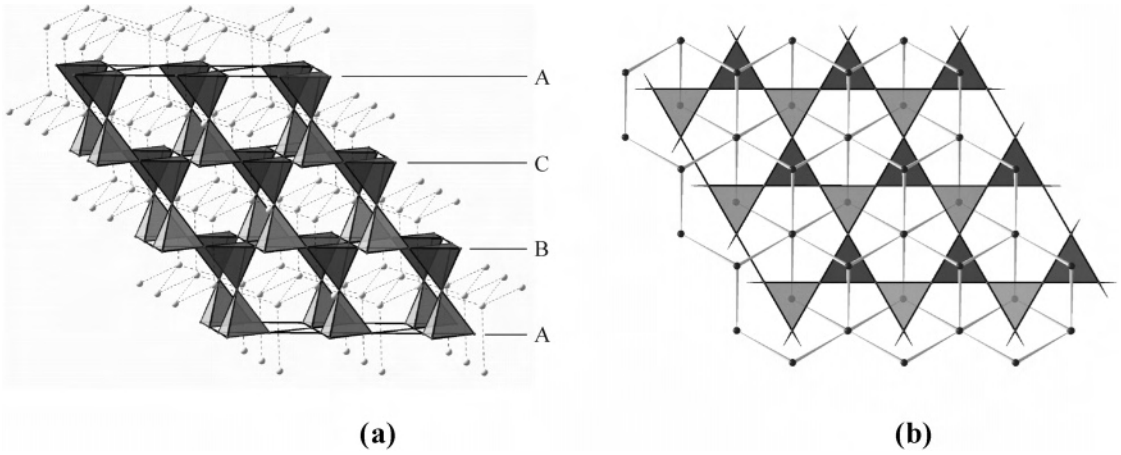

Figure 1. The structure of the Laves phase, KBi_2, represented (a) by the two partial structures, vertex-sharing tetrahedra of Bi atoms and diamond lattice of K atoms, and (b) the Kagomé net of Bi atoms, which form the cubic-type stacking sequence in shown in a. Tetrahedra depicted in light gray are larger in the structure of $F\bar{4}3m$ $KBi_{2-x}Pb_x$.

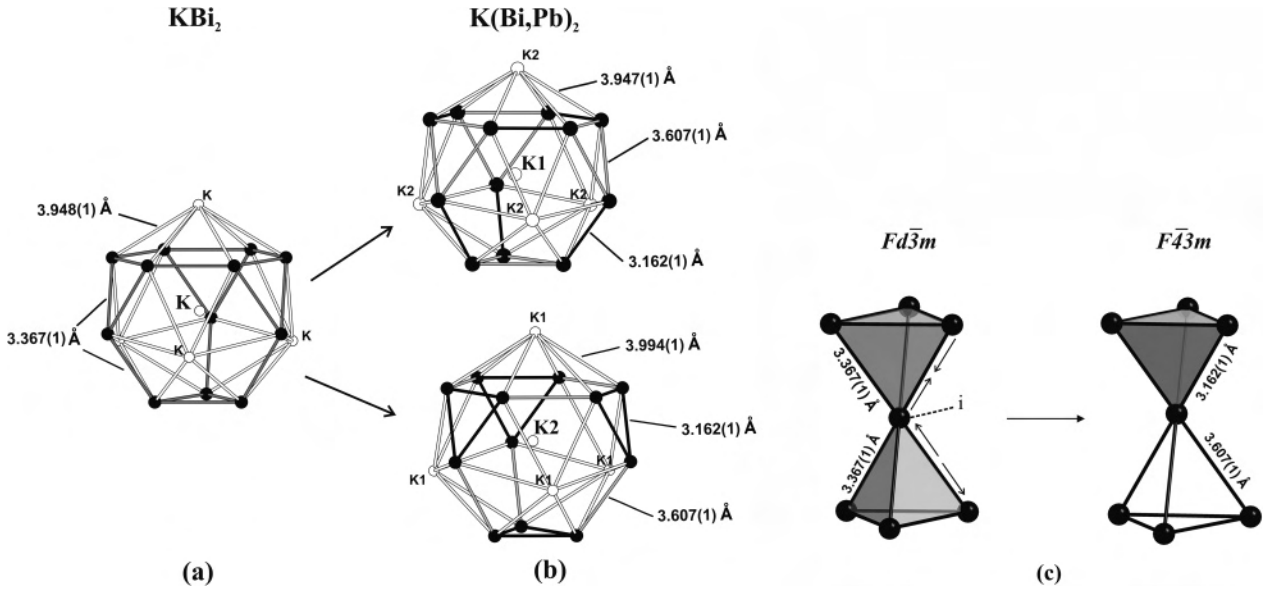

Figure 2. (a) Coordination polyhedron around the K atoms in KBi_2, (b) coordination polyhedra around the two different K atoms in $F\bar{4}3m$ $KBi_{2-x}Pb_x$, and (c) the distortion of two edge-sharing tetrahedra in $F\bar{4}3m$ $KBi_{2-x}Pb_x$ (right) from $Fd\bar{3}m$ KBi_2 (left).

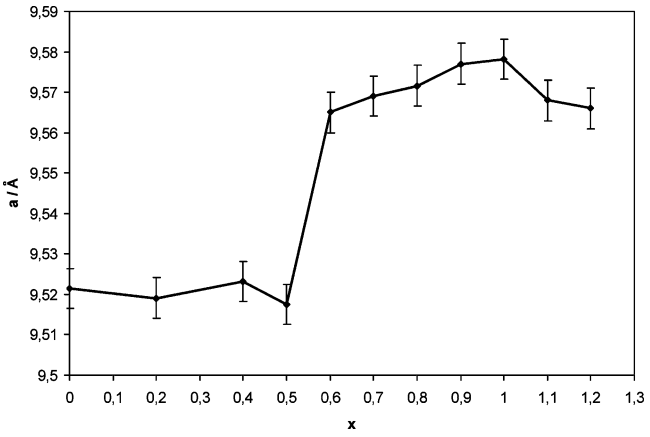

Figure 3. Evolution of the cubic lattice parameter of $KBi_{2-x}Pb_x$ as a function of x. The error bars correspond to the maximum standard deviation from the refinement of lattice parameters (±0.01 Å).

single 16-fold position. The splitting into two types of tetrahedra produces two different B−B distances (3.162 and 3.607 Å) compared to the single distance in KBi_2 (3.367 Å). Interestingly, the interatomic distances K1−B and K2−B in $KBi_{2-x}Pb_x$ remain very similar, but as a consequence of the two types of framework tetrahedra, the Friauf polyhedra around K1 and K2 are different (Figure 6). K1 coordinates exclusively the larger triangles and K2 the smaller ones.

In agreement with resistivity measurements,[15] magnetic measurements reveal that KBi_2 is an electric conductor. Investigations of the low-field temperature-dependent magnetic behavior show the typical curves for diamagnetic shielding and the Meissner effect of a superconductor. The sample is cooled without an external magnetic field below T_c. The application of an external field of 10 G leads to negative values for the magnetic susceptibility. The diamagnetic property of KBi_2 disappears at higher temperatures with the transition temperature at 3.5 K (on set). While the sample was cooled in the external field, a jump of the susceptibility is observed again (Figure 5). The plot indicates that KBi_2 is a first-order superconductor.

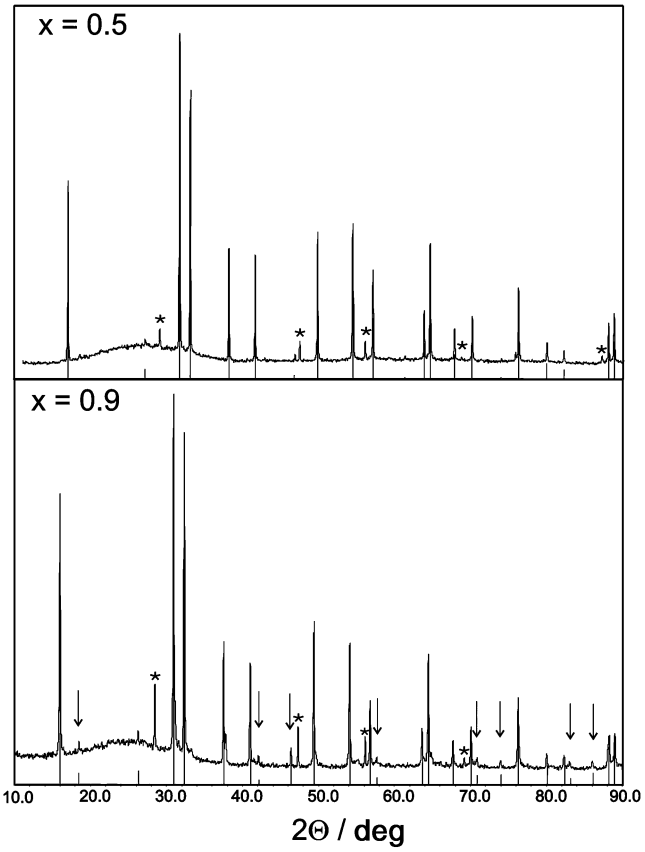

Figure 4. X-ray powder diffraction patterns of $KBi_{2-x}Pb_x$, (a) $x = 0.5$ and (b) $x = 0.9$. Arrows indicate extra reflections and Si peaks are highlighted by stars.

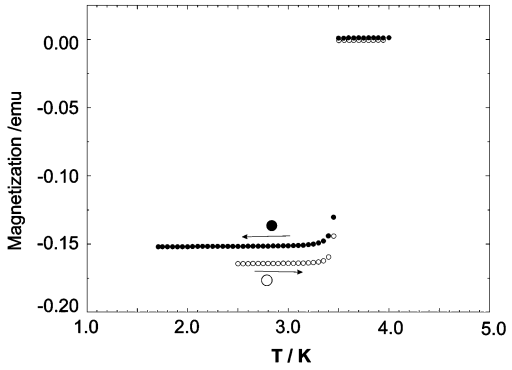

Figure 5. SQUID magnetic measurement of KBi_2. Diamagnetic shielding (○) and Meissner effect (●) as a function of temperature.

4. Discussion

The symmetry lowering, $Fd\bar{3}m \rightarrow F\bar{4}3m$, observed in $KBi_{2-x}Pb_x$ represents a unique structural distortion of the cubic Laves-phase structure $MgCu_2$. Although the $F\bar{4}3m$ structure is known as the $AuBe_5$-[17] or $MgSnCu_4$-structure type[18] and has been described as an ordered ternary Laves phase, its direct evolution from the $MgCu_2$ structure with the same A- and B-type components is unprecedented. The rigid B atom framework with all distances equal in $Fd\bar{3}m$ turns into a flexible one in $F\bar{4}3m$ with two different distances. We assume that the two 16-fold positions occupied by the

(17) Misch, L. *Metallwirtsch.* **1935**, *14*, 897.
(18) Osamura, K.; Murakami; Y. *J. Less-Common Met.* **1978**, *60*, 311.

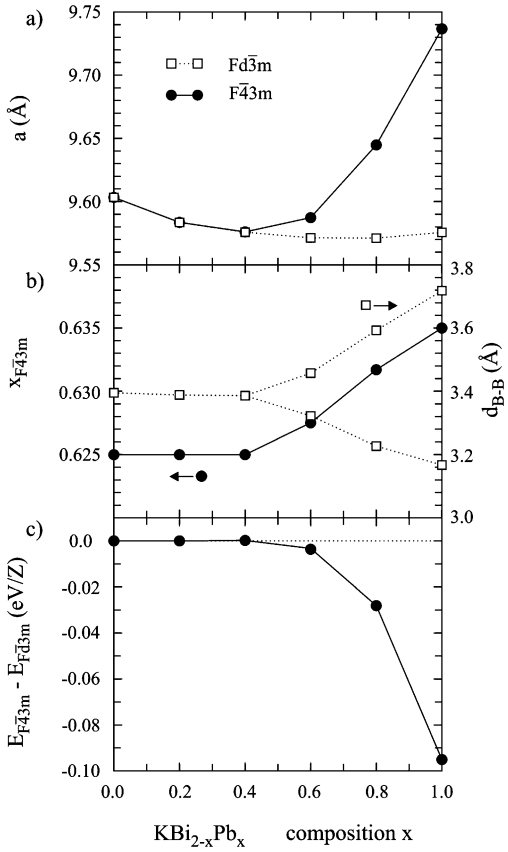

Figure 6. Summary of the computational structure optimization for $KBi_{2-x}Pb_x$: (a) evolution of the lattice parameter, (b) the atomic positional parameter of the Wyckoff site 16e (x,x,x) in $F\bar{4}3m$ together with the interatomic distances in the B atom framework, and (c) the structural energy difference with composition x.

B atoms, 16d and 16e in $Fd\bar{3}m$ and $F\bar{4}3m$, respectively, are randomly occupied by Bi and Pb atoms. However, we cannot rule out Bi/Pb ordering, which is invisible to X-ray diffraction, on the B atom framework. To understand the nature of the $Fd\bar{3}m \rightarrow F\bar{4}3m$ distortion and the homogeneity range of the $F\bar{4}3m$ phase, we performed first-principles calculations in which the Bi/Pb random occupational disorder was treated by VCA.

Figure 6 shows the result of the structure optimization for the system $KBi_{2-x}Pb_x$ in space groups $Fd\bar{3}m$ and $F\bar{4}3m$. We considered the compositions $x_{Pb} = 0$, 0.2, 0.4, 0.6, 0.8, and 1.0. For the high-symmetry $MgCu_2$-structure type ($Fd\bar{3}m$), the cubic unit cell parameter is the only structural variable. For binary KBi_2, we obtained a value of 9.603 Å. This is approximately 1% larger than the experimentally determined lattice parameter and corresponds to an overestimation of the ground-state volume by about 2.5%. Small overestimations of ground-state volumes (up to 5%) are frequently observed when using GGA for assessing exchange and correlation energy. With increasing Pb concentration, the lattice parameter varies only slightly. It first decreases to 9.57 Å, which is attained for compositions between $x_{Pb} = 0.6$ and 0.8, and after that increases to 9.577 Å for $x_{Pb} = 1.0$. Until a composition $x_{Pb} = 0.4$ the substitution of Bi by Pb is not recognized in a structural change. For $x_{Pb} = 0.6$, however, the lattice parameter of the $F\bar{4}3m$ structure

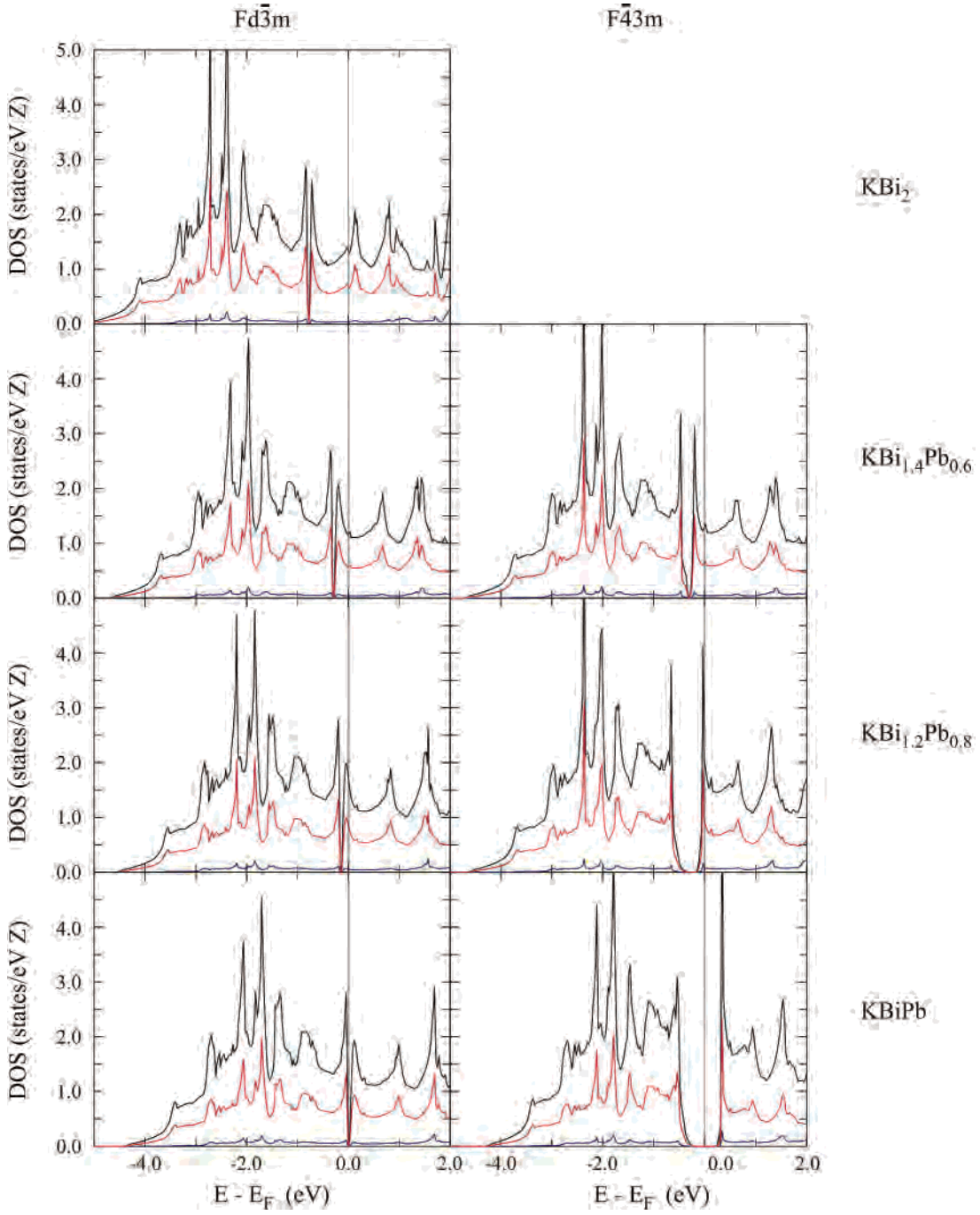

Figure 7. Density of states (DOS) for $KBi_{2-x}Pb_x$ in $Fd\bar{3}m$ (left panel) and $F\bar{4}3m$ (right panel) at selected compositions $x = 0$, 0.6, 0.8, 1.0. Black lines, total DOS; red lines, Bi/Pb p partial DOS; dark blue lines, K s,p partial DOS. The Bi/Pb 6s states are not shown. These states are well localized at about 9 eV below the Fermi level (vertical lines) and confined to a narrow energy range.

increases by 0.015 Å with respect to the high-symmetry $Fd\bar{3}m$ structure, and at the same time, the x positional parameter departs the ideal value of 0.625 and increases to 0.628. The onset of the structural distortion is accompanied by a slight decrease in the total energy. Above $x_{Pb} = 0.6$, the distortion increases drastically with increasing Pb concentration. At $x_{Pb} = 0.8$, the lattice parameter of the $F\bar{4}3m$ structure is larger by 0.074 Å, and at $x_{Pb} = 1.0$ it is larger by even 0.16 Å. For the latter composition, the x positional parameter becomes 0.635 and $F\bar{4}3m$ KBiPb reaches a substantial stabilization (0.095 eV/Z (9.2 kJ/mol)) over the high-symmetry structure.

The theoretical findings excellently mirror the experimental results. First, the constant behavior of the lattice parameter at lower Pb concentrations is well reproduced. Further, the experimentally observed lattice parameter increase of around 0.06 Å for $KBi_{2-x}Pb_x$ ($x \approx 0.8$) matches the calculated increase for $x_{Pb} = 0.8$, and the refined x positional parameter for a crystal with $x \approx 0.8$ takes a value of 0.6332, which is close to the calculated value for $x_{Pb} = 0.8$ (0.632). The immediate question is why does $x \approx 0.8$ represent, experimentally, the border composition for the $F\bar{4}3m$ phase, even though the theoretical calculations clearly show a further energy lowering over the $MgCu_2$ structure in an increasingly

distorted compound KBiPb ($x = 1.0$). To answer that question and to get some insight into the bonding of the $F\bar{4}3m$ phase, we analyzed the electronic structure for KBi$_{2-x}$Pb$_x$.

The electronic structure changes of KBi$_{2-x}$Pb$_x$ are compiled in Figure 7. This figure presents the electronic density of states (DOS) of the system at some selected compositions. For binary KBi$_2$, with the high-symmetry MgCu$_2$ structure, it can clearly be seen that the occupied valence bands have predominately Bi character; the K contribution to these bands is negligible. Thus, Bi appears reduced by electropositive K, and its three-dimensional network composed of vertex condensed tetrahedra can be considered as polyanionic. The DOS at the Fermi level attains a high value, which is in agreement with the good metallic conductivity of this compound. An important feature in the band structure of KBi$_2$ is a narrow but sharp pseudo gap at 0.8 eV below the Fermi level, which corresponds to the half filled p band. Upon Pb incorporation, the electronic structure of $Fd\bar{3}m$ KBi$_2$ displays a rigid-band behavior. This means that the exchange of Bi for Pb influences basically only the location of the Fermi level, which shifts toward the pseudo gap with increasing x_{Pb}. The onset of the structural change $Fd\bar{3}m \rightarrow F\bar{4}3m$ is recognized for $x_{Pb} = 0.6$ by a considerable widening of the pseudo gap, which for $x_{Pb} = 0.8$ opens up to a real band gap just below the Fermi level. Finally, for $x_{Pb} = 1.0$, the band gap has obtained a size of 0.35 eV, and the Fermi level coincides with its location. As a consequence, $F\bar{4}3m$ KBiPb turns into a semiconductor, and its electronic structure corresponds to that of a Zintl phase. The mechanism of the structural distortion $Fd\bar{3}m \rightarrow F\bar{4}3m$ in the KBi$_{2-x}$Pb$_x$ system resembles that of a Peierls distortion. The six equal nearest-neighbor Bi−Bi distances in the polyanionic network of the original Laves-phases KBi$_2$ split into a set of three short and three long distances. As a consequence, a band gap in the DOS is opened. The structural distortion and, thus, the size of the band gap become largest when the Fermi level coincides with the band gap (i.e., for the composition $x_{Pb} = 1.0$). This situation also yields the largest energy stabilization.

A further distinctive feature of the electronic structure for KBi$_{2-x}$Pb$_x$ is the pair of sharp singularities flanking the pseudo gap or band gap. These singularities occur in both the $Fd\bar{3}m$ and $F\bar{4}3m$ structures and correspond to flat bands. When the DOS for the $Fd\bar{3}m$ and $F\bar{4}3m$ phases with the same composition are compared, it is realized that the stabilization of the distorted $F\bar{4}3m$ structure is mainly the result of the lowering of the lower singularity with respect to the Fermi level upon widening of the pseudo gap/band gap. The location of the upper singularity (with respect to the Fermi level) is only slightly affected by the symmetry reduction. The upper singularity might be the reason for the experimental border composition $x \approx 0.8$ because slightly above a composition of $x = 0.8$, the Fermi level enters this singularity. A singularic DOS at the Fermi level indicates an electronic instability of the system, which could drive a phase segregation around this particular composition. Numerous preparative attempts to increase the Pb content in KBi$_{2-x}$Pb$_x$ above $x = 0.8$ were unsuccessful. The emergence of additional ternary phases, which could not be characterized yet, appears to suppress the formation of KBiPb.

The structural distortion $Fd\bar{3}m \rightarrow F\bar{4}3m$ in KBi$_{2-x}$Pb$_x$ is remarkable because it describes a continuous transition from a fully delocalized metallic Laves phase, KBi$_2$, to a proper (i.e., charge-balanced) semiconducting Zintl phase, KBiPb. In (hypothetical) KBiPb, the p band is half filled and according to the Zintl−Klemm concept the compressed tetrahedra may be regarded as separated entities, B_4^{2-}, in which each edge corresponds to a two-center two-electron bond. However, the compressed tetrahedra cannot be considered as separated noninteracting entities. The difference between the long and short distances in the B atom network of $F\bar{4}3m$ KBiPb is about 0.5 Å (cf. Figure 2c). A rather short separation of polyanionic clusters is frequently observed for Zintl phases containing heavy p-block elements. For example, in NaPb, which contains discrete electron-precise Pb_4^{4-} tetrahedra (tetragonal NaPb type) the interatomic distances within and between the clusters are 3.15 Å and 3.64 Å, respectively.[19] This is very similar to the situation in KBiPb.

We recently reported that KBi$_2$ is also formed by precipitation from filtered ethylenediamine solutions of K and Bi; thus, the ionic contribution is expected to be as important as the metallic interactions in the typical intermetallic Laves-phase KBi$_2$.[20] The present investigation supplements those intriguing observations. KBiPb is an electron-precise Zintl phase containing tetrahedral $(Bi_2Pb_2)^{2-}$ with Bi and Pb atoms randomly distributed over the four positions of the tetrahedra. Whereas these Zintl anions have not yet been isolated from solutions, the iso(valence) electronic anions $(Sn_2Bi_2)^{2-}$ and $(Pb_2Sb_2)^{2-}$ with random distribution of the atoms are known.[21]

5. Conclusions

CaAl$_2$, KPb$_2$, and ABi$_2$ (A = K, Rb, Cs) are distinguished main-group metal Laves phases. The rather large electronegativity difference of the constituting atoms puts these systems at the border to charge-balanced Zintl phases. Electron concentration is a crucial factor determining which of the three structures, MgCu$_2$, MgZn$_2$, and MgNi$_2$, is adopted in Laves-phase-forming systems. This has been known for transition metal Laves phases[22] and has also been recently established for s−p-bonded Laves-phase systems.[3]

The pseudobinary system CaAl$_{2-x}$Mg$_x$ displays the Laves-phase structural sequence MgCu$_2$ → MgNi$_2$ → MgZn$_2$ with increasing x (i.e., decreasing electron concentration). A similar behavior was expected for KBi$_{2-x}$Pb$_x$. However, our investigation of this system revealed a peculiar distortion, $Fd\bar{3}m \rightarrow F\bar{4}3m$, of the cubic MgCu$_2$ structure adopted by KBi$_2$ when replacing Bi with Pb. For KBi$_{2-x}$Pb$_x$, the decreasing electron concentration does not result in the formation of the MgNi$_2$ structure but in a continuous

(19) Marsh, R. E.; Shoemaker D. P. *Acta Crystallogr.* **1953**, *6*, 197.
(20) Kuznetsov, A. N.; Fässler, T. F. *Z. Anorg. Allg. Chem.* **2002**, *628*, 2537−2541.
(21) Critchlow, S. C.; Corbett, J. D. *Inorg. Chem.* **1982**, *21*, 3286. Critchlow, S. C.; Corbett, J. D. *Inorg. Chem.* **1985**, *24*, 979.
(22) Johnston, R. L.; Hoffmann, R. *Z. Anorg. Allg. Chem.* **1992**, *616*, 105.

transition to a charge-balanced Zintl phase, which is reached for a composition KBiPb. Experimentally, it was not possible to assess the semiconducting end-member of this transition. The maximum Pb content of $F\bar{4}3m$ $KBi_{2-x}Pb_x$ was found to be approximately 0.8. Attempts to increase the Pb content resulted in the formation of additional ternary phases. This manifests a general problem with the investigation of quasibinary systems. The number of possible phase relations is greatly enhanced in ternary systems, and products with a desired quasibinary stoichiometry may not form for certain compositional ranges. Interestingly, the compounds $AePb_2$ (Ae = Ca, Sr, Ba), which formally would match the electron count of the new Zintl-phase structure $F\bar{4}3m$ KBiPb, are also not known. Thus, it appears to be a challenge to prepare a charge-balanced Zintl phase with the $F\bar{4}3m$ structure of KBiPb.

Acknowledgment. U.H. acknowledges support by the Swedish Research Council (VR).

Supporting Information Available: X-ray crystallographic files in CIF format. This material is available free of charge via the Internet at http://pubs.acs.org.

IC050603H